Babol University of Medical Sciences
IJMCM
International Journal of Molecular and Cellular Medicine
p-ISSN: 2251-9637 o-ISSN: 2251-9645
Cellular and Molecular Biology Research Center

Mesenchymal Stem Cells Therapy Led to the Improvement of Spatial Memory in Rats with Alzheimer's disease Through Changing the Expression of LncRNA TUSC7/ miR-449a/ PPARγ and CD36 Genes in the Brain Tissue

Seyedeh Pardis Pezeshki[1,2], Mehrnaz Karimi Darabi[1], Zahra Nazeri[1], Alireza Sarkaki[3], Mojtaba Rashidi[1], Hossein Babaahmadi-Rezaei[4], Alireza Kheirollah[1,5], Maryam Cheraghzadeh[1,6*]

1. Department of Biochemistry, School of Medicine, Ahvaz Jundishapur University of Medical Sciences, Ahvaz, Iran.
2. Student Research Committee, Ahvaz Jundishapur University of Medical Sciences, Ahvaz, Iran.
3. Department of Physiology, Medicine Faculty, Ahvaz Jundishapur University of Medical Sciences, Ahvaz, Iran. Persian Gulf Physiology Research Center, Medical Basic Sciences Research Institute, Ahvaz Jundishapur University of Medical Sciences, Ahvaz, Iran.
4. Hyperlipidemia Research Center, Department of Clinical Biochemistry, Faculty of Medicine, Ahvaz Jundishapur University of Medical Sciences, Ahvaz, Iran.
5. 548-E Borwell Research Building, Geisel School of Medicine at Dartmouth, Hanover, NH 03755, USA.
6. Persian Gulf Physiology Research Center, Medical Basic Sciences Research Institute, Ahvaz Jundishapur University of Medical Sciences, Ahvaz, Iran.

Article type:
Original Article

Received:
2023.10.02
Revised:
2023.10.31
Accepted:
2023.11.11

ABSTRACT

Mesenchymal stem cells (MSCs) have the ability to phagocytize amyloid beta (Aβ) plaques and lower inflammation through the activity of microglia. Peroxisome proliferator-activated receptor gamma (PPARγ) is a protein involved in reducing inflammation through the activity of microglia and the phagocytosis of Aβ plaques by scavenger receptor CD36, in this study, the effect of MSCs therapy on memory function and plaques was investigated. A total of 24 adult male Wistar rats were randomly divided into three groups:1) the control group, 2) the Aβ-treated group (Alzheimer's disease (AD)), and 3) the MSC-treated group (AD + MSC). After the treatment with Aβ and MSCs, western blotting and real-time polymerase chain reaction (PCR) techniques were used to assess protein and gene expression levels, respectively. MSCs improved spatial learning and memory in the AD group ($p \leq 0.05$). The expression levels of PPARγ, lncRNA TUSC7, and CD36 genes were significantly elevated in the group receiving MSCs compared to the AD group ($p \leq 0.0001$). Also, the expression level of miR-449a significantly decreased in the AD + MSC group ($p \leq 0.0001$). Moreover, western blot analysis revealed that PPARγ and CD36 protein levels were enhanced in the AD + MSC group compared to the AD group ($p \leq 0.0001$). MSC treatment led to the positive regulation of the PPARγ gene and its protein expression by ncRNAs, which could have a beneficial impact on CD36 protein levels, and subsequently, reduce the number of plaques in the cell recipient.

Keywords: Alzheimer's disease, stem cells, PPAR gamma, microRNAs, LncRNA

Cite this article: Pezeshki P, *et al*. Mesenchymal Stem Cells Therapy Led to the Improvement of Spatial Memory in Rats with Alzheimer's disease Through Changing the Expression of LncRNA TUSC7/ miR-449a/ PPARγ and CD36 Genes in the Brain Tissue. *International Journal of Molecular and Cellular Medicine. 2023; 12(2):108-119.* **DOI:** 10.22088/IJMCM.BUMS.12.2.108

*Corresponding: Maryam Cheraghzadeh
Address: Persian Gulf Physiology Research Center, Medical Basic Sciences Research Institute, Ahvaz Jundishapur University of Medical Sciences, Ahvaz, Iran.
E-mail: cheraghzade_m@ajums.ac.ir

Introduction

Alzheimer's disease (AD) was first introduced more than a century ago in 1907. Since then, the number of patients suffering from this condition has continued to rise significantly (1). The key pathological characteristic of AD is the accumulation of amyloid beta (Aβ) peptides, which are believed to cause synaptic damage and cognitive impairment in AD patients. These peptides are produced via the cleavage of the amyloid precursor protein (APP) and their accumulation results from excessive generation and defects in their clearance pathways (2). Peroxisome proliferator-activated receptors (PPARs) belong to the nuclear hormone receptor (NHR) family and are implicated in neuroprotection, stem cell preservation, and protection against inflammation (3). PPARγ serves a crucial function in Aβ clearance, leading to the reduction of neuroinflammation caused by Aβ in the brain tissue (4). Moreover, PPARγ activation increases microglial phagocytosis of Aβ by the scavenger receptor CD36, which reduces Aβ levels in the cerebral cortical and hippocampal areas (5). CD36 is a membrane glycoprotein that belongs to the B2 class of scavenger receptors (SCARB-2). The CD36 receptor is expressed on the surface of microglial cells (the primary phagocytic cells), as well as astrocytes, and can bind to $A\beta_{1-40}$ and $A\beta_{1-42}$ fragments. The binding of these proteins to the CD36 receptor promotes phagocytosis (6, 7). The expression of these proteins is affected by several factors, including non-coding RNAs (ncRNAs), such as TUSC7 and miR-449a. Long non-coding RNAs (lncRNAs) are a subgroup of ncRNAs that are longer than 200 nucleotides (nt). LncRNAs affect AD pathogenesis with their diverse biochemical and functional roles, including chromatin modification, as well as post-transcriptional and post-translational regulation (8). MiRNAs are small ncRNAs that regulate gene expression by binding to the 3′ untranslated region (3'UTR) of mRNA. MiRNAs have also been recognized as biomarkers for AD (9, 10). MiR-449a can negatively affect PPARγ expression whereas lncRNA TUSC7 can increase PPARγ expression by reducing miR-449a (11). Due to the progressive nature of AD, identifying biological markers is crucial for early diagnosis. Although there is no definitive treatment for AD, stem cells are recommended for therapeutic approaches due to their capacity for self-renewal, proliferation, and differentiation (12). The aim of cell therapy in AD patients is to either replace damaged tissue cells or mitigate the damaging effects of the disease on brain tissue (13). Since mesenchymal stem cells (MSCs) can be obtained from different sources and have the ability to differentiate into various cell lines, they have attracted the attention of researchers due to their possible application in AD treatment (14, 15). Neurotrophic factors produced by MSCs affect the phagocytosis of Aβ plaques and reduce brain inflammation through microglia (16, 17).

The present study aimed to investigate the effect of MSC therapy on the elimination of Aβ plaques in rats with AD (Figure 1). Therefore, the effect of this approach on the expression levels of PPARγ (an effective factor in removing Aβ plaques), CD36 (a downstream protein activated by PPARγ in the process of clearing plaques), miR-449a, and lncRNA TUSC7 (upstream regulatory factors of PPARγ) genes along with the expression levels of PPARγ and CD36 proteins was studied in the brain tissue of rats with Aβ-induced AD.

Materials and methods

Animals

[DOI: 10.22088/IJMCM.BUMS.12.2.108]

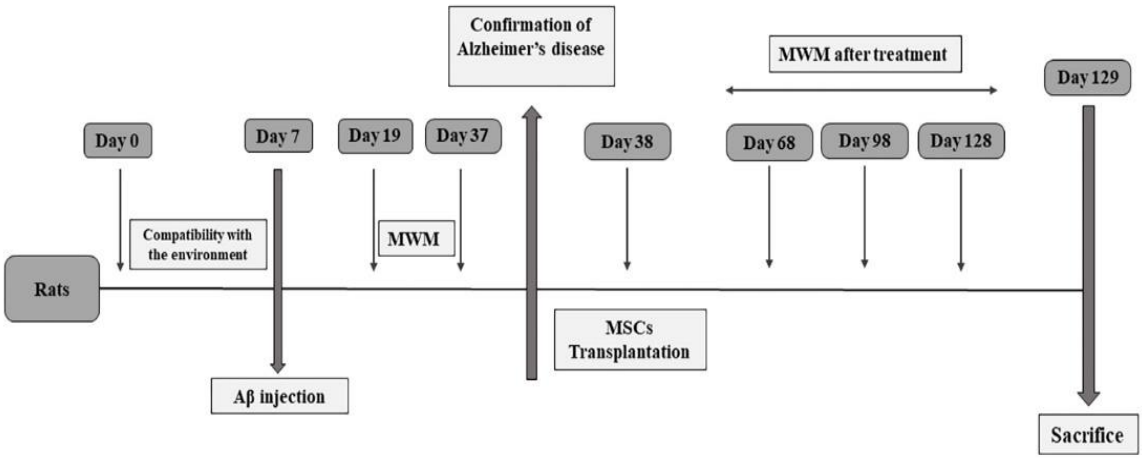

Fig.1. Flowchart of the study design.

A total of 24 adult male Wistar rats weighing between 250 and 300 g were acquired from the Animal Center of Jundishapur University of Medical Sciences in Ahvaz, Iran. The rats were randomly divided into three groups of eight and maintained under standard conditions with a temperature of 21–23°C, 55% humidity, and a 12-h light/dark cycle. They also had free access to rodent food and tap water. The groups were as follows: The control group (n = 8), which received 2.5 µL of phosphate-buffered saline (PBS); the AD group (n = 8), which was treated with Aβ to induce neurotoxicity and cognitive impairment; 3) the AD + MSC group (n = 8), which was treated with MSCs after the induction of AD. All procedures involving animal studies were conducted in accordance with the ethical standards set by the local Ethics Committee of Ahvaz Jundishapur University of Medical Sciences (IR.AJUMS.ABHC.REC.1401.015).

Induction of neurotoxicity and cognitive disorders by Aβ

First, $A\beta_{1-42}$ (Sigma Aldrich, USA) was dissolved in PBS and stored at -70°C until use. Before use, $A\beta_{1-42}$ was incubated for five days at 37°C to convert it from its monomeric state to the more toxic peptide. The animals in the AD group were anesthetized through an intraperitoneal injection of ketamine and xylazine (90:10 mg/kg) (18) and fixed in a stereotaxic apparatus with their head hair shaved. After splitting the dorsal skin on their heads, Aβ was bilaterally injected at a concentration of 5 µM and a rate of about 1 µL/min into the anterior hippocampus (CA1 region) of the AD group (Anteroposterior (AP) = -4.30 mm, Mediolateral (ML) = ± 2.4, and Dorsoventral (DV) = 2.6 mm) using a 10-µL Hamilton syringe according to the Paxinos and Watson rat brain atlas. The solution was allowed to remain in place for 10 min to prevent re-entry into the syringe (19).

Morris water maze (MWM)

This test was used to assess memory and spatial learning in rats. In the MWM test, a swimming pool (140 cm in diameter and 80 cm in height) was filled to a depth of 60 cm with water at a temperature of 25 ± 1°C. The pool was divided into four equal quadrants: north (N), south (S), west (W), and east (E). This test was carried out four weeks after the induction of neurotoxicity and cognitive impairment in the rats via Aβ treatment. The animals were examined for four consecutive days, with four training sessions per day (20).

[DOI: 10.22088/IJMCM.BUMS.12.2.108]

According to the protocol, each animal was randomly placed in one of the quadrants and allowed to swim for 60 s to locate and climb onto the hidden escape platform. After finding the platform, the animal was allowed a 30-s rest before the next trial. The time taken to find the platform (latency), the swimming distance (path length), and the swimming speed were recorded. On the fifth day, a probe trial was conducted to evaluate memory retrieval. During this trial, the hidden platform was removed and the percentage of time spent in the goal quadrant (where the platform was located in the learning phase) was recorded during a single swimming trial. This test was carried out for all the studied groups. The MWM test was conducted after four weeks of MSC injection in the AD + MSC group according to the previous protocol.

Cell isolation, characterization, and injection into animals

To prepare MSCs, rat epididymal fat tissue was employed. The isolated fat tissue was placed on ice in a container with PBS, PenStrep, and amphotericin. The tissue was crushed and washed three times with PBS, before being mechanically digested with collagenase IV. The obtained cells were transferred into 75-mL flasks and placed in an incubator at 37°C with a 5% CO_2 concentration. The cells were passaged when they reached a density of 70%, and after two passages and achieving the appropriate morphology, they were injected into the animals in the AD + MSC group. In addition, to verify that the cultured cells were stem cells, flow cytometric analysis was performed to assess the expression levels of CD45, CD34, CD44, and CD90 markers. To evaluate the potential of the extracted cells to differentiate into adipocyte and osteoblast cell lines, the standard differentiation and staining method was used according to the protocol (21). Finally, 1×10^6 MSCs were dissolved in 10 µL of PBS (22) and injected into both sides of the brain ventricles of the animals in the AD + MSC group (AP = -1.20 mm, ML = ±2 mm, and DV = 3.8 mm).

Animal sacrifice and brain extraction

After conducting the behavioral tests, the rats of each group were irreversibly anesthetized with an overdose of sodium pentobarbital (Nesdonal 80 mg/kg, IP). The anesthetized rat was positioned on its back on the surgical tray, and its chest was cut open using surgical scissors. A 22 G perfusion needle was inserted into the left ventricle, and shortly after, a small incision was made in the right atrium. The perfusion fluid was drained from the body, and after the liver was clear, the brain was quickly removed.

Congo red staining

Aβ deposits were identified using Congo red staining. The deeply anesthetized rats of each group were sacrificed, and tissue samples from the hippocampus and cortex of their brains were isolated, fixed, and stained using the FarTest Congo red staining kit (Farzaneh Arman CO, Iran). Finally, a cover glass was mounted on the stained slide.

Western blot

After washing the brain samples with PBS, lysis buffer was used to homogenize the tissues. Total protein levels were determined using the Bradford method, and 100 µg of each sample was assessed using 12% sodium dodecyl sulfate-polyacrylamide gel electrophoresis (SDS-PAGE). Proteins were transferred to a polyvinylidene fluoride (PVDF) membrane and blocked with 5% skimmed milk in transfer buffer (Tris-buffered saline, TBS). Immunoblots were visualized using a dilution of mouse anti-rabbit IgG-horseradish peroxidase (HRP) (Santa Cruz Biotechnology, USA) and the chemiluminescence western blotting substrate. Densitometric analysis was performed using JS 2000 device software (BonninTech, China).

[DOI: 10.22088/IJMCM.BUMS.12.2.108]

Evaluation of PPARγ, lncRNA TUSC7, and CD36 mRNAs using real-time polymerase chain reaction (PCR)

RNA extraction was conducted using the Pars Toos RNA extraction kit according to the manufacturer's protocol. To synthesize cDNA from the extracted RNA, the Pars Toos cDNA synthesis kit (Easy cDNA Synthesis Kit) was employed according to the manufacturer's instructions. To perform real-time PCR, specific primers for PPARγ, lncRNA TUSC7, and CD36 genes, as well as cDNA and SYBR Green PCR Master Mix, were used (Table 1). Moreover, the hypoxanthine-guanine phosphoribosyltransferase (HPRT) gene was applied as an internal control, and the relative change in the expression of the mentioned genes was calculated using the ΔΔCT method.

Table 1. Specific primers for studied genes.

Gene	Primer	Length
PPAR$\boldsymbol{\gamma}$	(F). 5'-CCGAAGAACCATCCGATTGAA-3' (R). 5'-AACCTGATGGCATTGTGAGAC-3'	141
TUSC7	(F). 5'-GTGGACCATGGCAACACAAA-3' (R). 5'-ACAGTGTGGTTAAGGAGCCG-3'	20
CD36	(F). 5'-TGCGACATGATTAATGGCACAG-3' (R). 5'-ACAGCATAGATGGACCTGCAA-3'	107
HPRT	(F). 5'-ACAGGCCAGACTTTGTTGGA-3' (R). 5'-TGGCTTTTCCACTTTCGCTG -3'	123

F: Forward; R: Reverse

Evaluation of miR-449a expression by real-time PCR

MiRNA isolation, cDNA synthesis, and miR expression analysis were conducted using commercially available kits (TIANGEN Co, China) according to the manufacturer's instructions. Synthesis of cDNA from miR was carried out using the poly A method. To perform real-time PCR, specific primers for miRNA-449a (listed in Table 2), the synthesized cDNA, SYBR Green, PCR master mix, and U6 (as the internal reference) were utilized.

Table 2. Specific primer for studied miR.

MicroRNA	Primer
U6	(F). 5'-CTCGCTTCGGCAGCACA -3' (R). 5'-AACGCTTCACGAATTTGCGT-3'
miR-449a	(F). 5'-AGATGGCAGTGTATTGTT-3'

F: Forward; R: Reverse

Statistical analysis

All statistical analyses were performed using GraphPad Prism 9.4.1 and IBM SPSS Statistics version 27.0. The results of all analyses were reported as mean ± standard deviation (SD). The three studied groups were compared using a one-way analysis of variance (ANOVA) test while MWM data were analyzed using two-way ANOVA followed by Tukey's post-hoc test. Correlation between PPARγ, lncRNA TUSC7 genes and miR-449a was investigated by Pearson correlation test. The significance level was considered to be $p<0.05$.

[DOI: 10.22088/IJMCM.BUMS.12.2.108]

Results

Characteristics of isolated cells

Seven days after the isolation and cultivation of rat adipose tissue cells, cell morphology was evaluated (Figure 2). In addition, the results of flow cytometric analysis are displayed in Figure 3. To investigate the differentiation potential of the cells isolated from adipose tissue, differentiation into adipocyte and osteoblast cell lines was induced (Figure 2). The results confirmed that the extracted cells were mesenchymal and pluripotent.

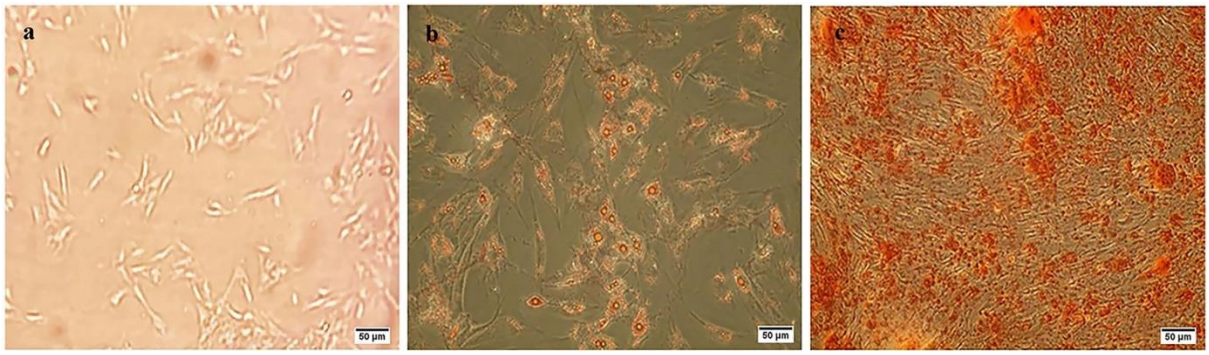

Fig.2. Cells isolated from rat adipose tissue. On the seventh day (×4) (a), differentiation into the adipocyte cell line (b), differentiation into the osteoblast cell line (c).

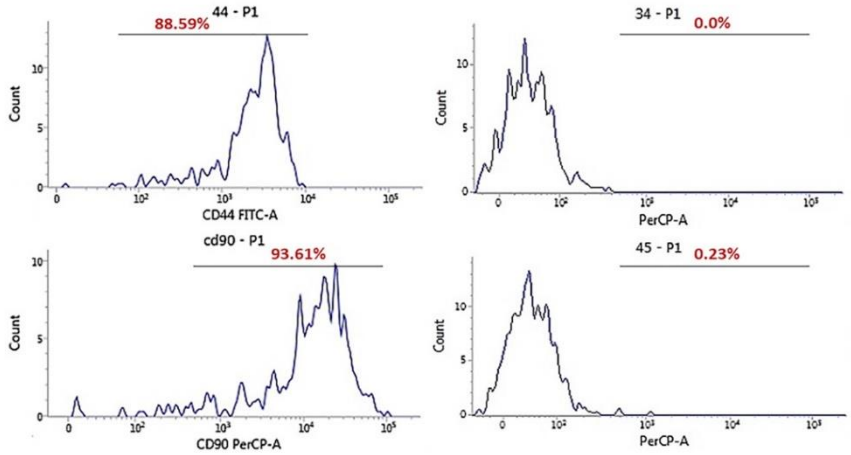

Fig.3. Flow cytometry test results. CD45 and CD34 as hematopoietic markers showed very low expression while CD44 and CD90 (mesenchymal markers) showed high expression.

Spatial learning and memory in MWM test

Four weeks after the injection of Aβ into the animals' anterior hippocampus (CA1 region), impairment in spatial learning and memory was observed. According to Figure 4A, the time spent to locate the hidden platform (latency time) had a significant increase in the AD group compared to the control group ($p < 0.0001$). Moreover, a significant decrease in the latency time was observed in the AD + MSC group compared to the AD group ($p < 0.0001$ and $p < 0.05$ for the first two days and the second two days, respectively). As indicated in Figure 4B, the percentage of time spent in the target quadrant during the probe trial significantly decreased in the AD group compared to the control group ($p < 0.0001$). However, the percentage of time spent in the

[DOI: 10.22088/IJMCM.BUMS.12.2.108]

target quadrant in the AD + MSC group significantly increased compared with the AD group ($p < 0.05$). The swimming speed was not different between all the studied groups. Therefore, it can be concluded that stem cell therapy led to improved memory and learning in the MSC-receiving group.

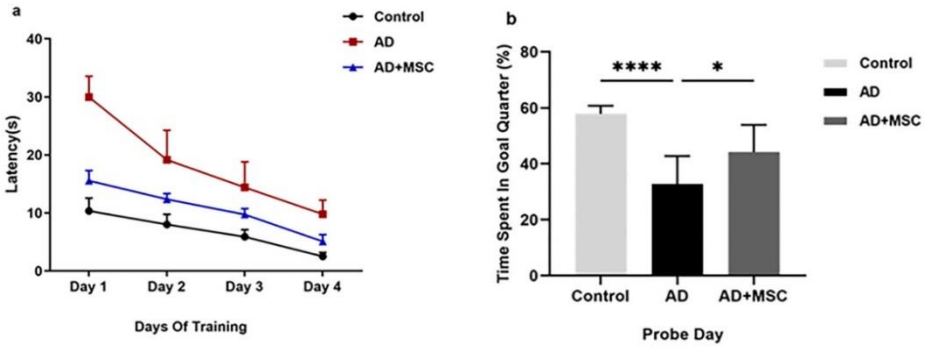

Fig.4. The effect of Aβ and MSCs on the spatial learning and memory of all three groups. Figure 4a shows the latency time in the spatial learning test on training sessions, which is significantly higher in AD compared to the control group. Moreover, this time significantly reduced in rats receiving MSCs compared to the AD group. Figure 4b shows the time spent in the target quadrant on the memory testing day (probe trial) significantly reduced in the AD group. On the other hand, this time significantly increased in AD + MSC group compared to the AD group. * $p \leq 0.05$, ** $p \leq 0.01$, *** $p \leq 0.001$, **** $p \leq 0.0001$.

Congo red staining

After conducting the behavioral tests and confirming AD induction, the animals' behavior was examined following MSC administration. The rats were sacrificed under irreversible anesthesia, and slides with Congo red staining were prepared from their brain samples. According to Figure 5, the level of Aβ plaques in the AD group was higher than in the control group, while it was significantly lower in the AD + MSC group than in the AD group.

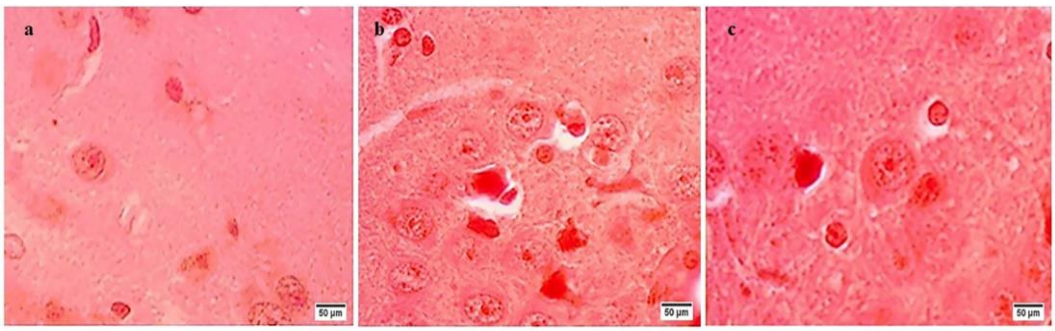

Fig.5. Preparation of brain tissue slices with Congo red staining to visualize Aβ plaques. The control group (a). The AD group (b). The AD + MSC group (c).

Confirming the correlation between PPARγ, lncRNA TUSC7 and miR-449a with Pearson's correlation test

According to the results obtained from Pearson's correlation test by SPSS software, As shown in Table 3, there was a direct significant correlation between lncRNA TUSC7 and PPARγ ($r=0.987$, $N=24$, $p <0.01$) and there was an inverse significant correlation between lncRNA TUSC7, PPARγ and miR-449a ($r= -0.980$, -0.989 respectively, $N=24$, $p <0.01$), which meant that higher expression of lncRNA TUSC7 was associated with higher expression of PPARγ and lower expression of miR-449a.

[DOI: 10.22088/IJMCM.BUMS.12.2.108]

Alterations in the expression levels of PPARγ, lncRNA TUSC7, CD36, and miR-449a genes

As shown in Figure 6 (Figures 6A-D), the expression level of PPARγ and lncRNA TUSC7 genes significantly decreased in the AD group compared to the control group while in the AD + MSC group, the expression level of both genes significantly increased. In addition, the level of CD36 gene expression significantly increased in both AD and AD + MSC groups compared to the control group ($p \leq 0.0001$). Moreover, the expression level of miR-449a in the AD group was significantly higher than in the control group, whereas it was significantly lower in the AD + MSC group compared to the AD group ($p \leq 0.0001$).

Table 3. Results of Pearson's correlation test

Correlations				
		Mir-449a	**lncTUSC7**	**PPARγ**
Mir-449a	Pearson Correlation	1	-.980**	-.989**
	Sig. (2-tailed)		.000	.000
	N	24	24	24
lncTUSC7	Pearson Correlation	-.980**	1	.987**
	Sig. (2-tailed)	.000		.000
	N	24	24	24
PPARγ	Pearson Correlation	-.989**	.987**	1
	Sig. (2-tailed)	.000	.000	
	N	24	24	24

**A significant difference ($p < 0.01$).

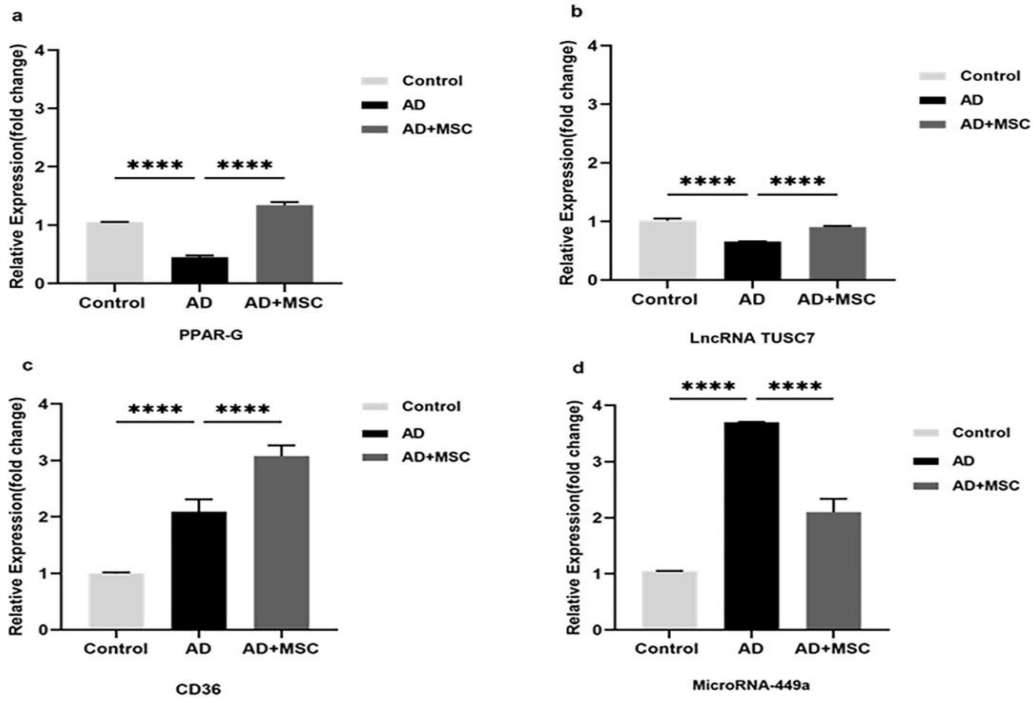

Fig.6. The expression level of the target genes in all three groups. The relative expression of the PPARγ (a). LncRNA TUSC7 relative expression (b). The expression level of CD36 (c). The expression of miR-449a (d). * $p \leq 0.05$, ** $p \leq 0.01$, *** $p \leq 0.001$, **** $p \leq 0.0001$.

[DOI: 10.22088/IJMCM.BUMS.12.2.108]

Alterations in the protein levels of PPARγ and CD36 in the studied groups

After evaluating the expression of the PPARγ gene and its downstream gene CD36, the protein levels of these two genes were determined using the western blot technique (Figure 7). It was found that the expression level of the PPARγ protein was significantly lower in the AD group than in the control group, while it was significantly higher in the AD + MSC group compared to the AD group ($p \leq 0.0001$). In addition, the expression of the CD36 protein significantly increased in the AD group compared to the control group, and a significant increase in the levels of this protein was also observed in the AD + MSC group compared to the AD group ($p \leq 0.0001$).

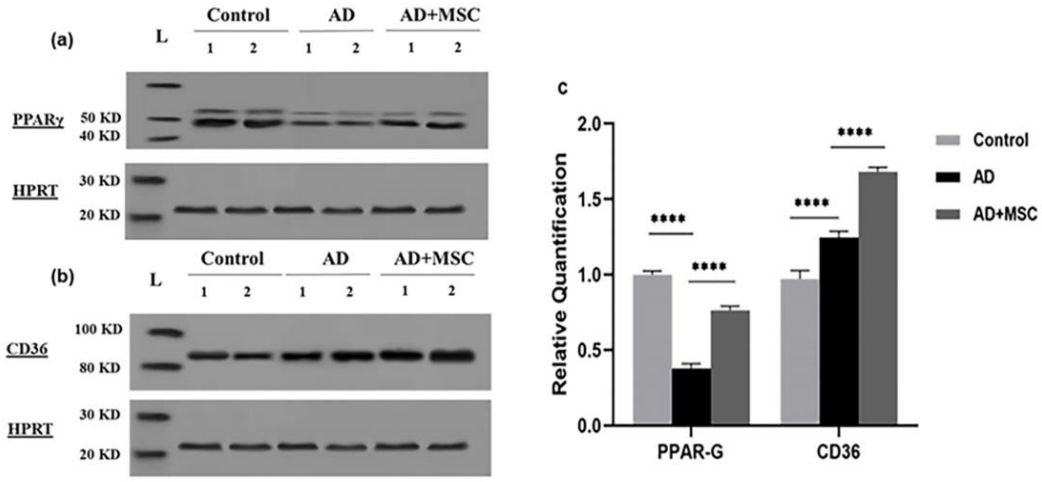

Fig.7. The effect of AD induction with Aβ and treatment of AD rats with MSC on PPARγ and CD36 proteins expression in rat brain tissue. PPARγ protein level in the AD group was significantly lower than the control group, and it was significantly higher in the AD + MSC group compared to the AD group (a). The level of CD36 protein in the AD group showed a significant increase compared to the control group, and it significantly increased in the AD+MSC group compared to the AD (b). * $p \leq 0.05$, ** $p \leq 0.01$, *** $p \leq 0.001$, **** $p \leq 0.0001$.

Discussion

Given the role of PPARγ as a key factor in the removal of Aβ plaques and considering the promising results of stem cell therapy in treating various diseases over the past few years, we investigated the effect of MSC therapy on the PPARγ protein, CD36 as its upstream factor and TUSC7 and miR-449a as downstream factors, in rats with Aβ-induced AD. In this study, three groups of rats were examined (Control, AD and AD + MSC), and neurotoxicity was induced via Aβ injection in two of the groups (AD and AD + MSC). Significant disparities in the expression of PPARγ and its regulatory factors were noted among the groups under investigation.

The results of the Morris Water Maze (MWM) test indicated that following the administration of amyloid beta, a significant disruption in learning and memory function was observed within the affected group. However, upon the subsequent injection of mesenchymal stem cells (MSCs), the AD + MSC group demonstrated improved conditions, with a significant amelioration of the behavioral disorder ($p \leq 0.0001$). This notable improvement is likely attributed to the characteristics of mesenchymal stem cells, as they effectively prevented brain cells apoptosis, facilitated increased proliferation and differentiation in the

[DOI: 10.22088/IJMCM.BUMS.12.2.108]

transplanted region, and promoted cognitive improvement by producing neurotrophic factors such as Brain-derived neurotrophic factor (BDNF), Beta-nerve growth factor (β-NGF), and Insulin-like growth factor-1 (IGF-1)(23).

Analysis of PPARγ gene expression and protein levels revealed a significant decrease in this protein within the AD group compared to the control group ($p < 0.0001$), potentially attributed to microglial damage during the course of Alzheimer's disease in rats. Following the treatment of AD group rats with mesenchymal stem cells, both the expression of PPARγ mRNA and protein exhibited a substantial increase compared to the AD group ($p \leq 0.0001$). This observation strongly underscores the positive influence of MSCs in augmenting or reactivating amyloid-beta clearance mediated by microglia. Moreover, this finding is corroborated by Congo red staining data.

It was observed that the expression levels of lncRNA TUSC7 was lower in the AD group compared to the control group, while the expression of miR-449a was higher in the AD group. The reduction in LncRNA expression can be ascribed to the adverse impacts of Aβ-induced inflammation and neurotoxicity on the regulatory pathways governing PPARγ gene expression. Furthermore, the upregulation of miR-449a is likely a consequence of the regulatory influence exerted by LncRNA TUSC7 on this microRNA. Notably, statistical analyses unveiled a correlation between the expressions of these three genes, suggesting that they operate within a regulatory axis capable of influencing the clearance of beta amyloid plaques. Conversely, in the cell-receiving group, there was an upregulation in the expression of lncRNA TUSC7 compared to the AD group and this increase resulted in a decrease in the expression of miR-449a. Ultimately, these changes culminated in an augmentation of both PPARγ gene and protein levels in the cell-receiving group ($p \leq 0.0001$). Notably, this study was the first to document the impact of MSC on the lncRNA TUSC7/ miR-449a / PPARγ axis in AD rat model, thereby triggering the stimulation of the amyloid plaque clearance pathway via PPARγ (5,11).

In the AD group, the expression level of CD36 increased, which may be due to Aβ injection. Since CD36 is known as a receptor for insoluble and aggregated Aβ, a rise in Aβ levels can lead to an increase in CD36 levels. Given that CD36 is mainly expressed in brain macrophages (microglia), this increase can result in the migration of microglia toward amyloid deposits, leading to inflammation and the phagocytosis of plaques. Moreover, the expression of CD36 showed a greater increase in the AD+MSCs compared to the AD group, which is likely due to the elevated expression of PPARγ and its role in CD36 activation. The escalation in the CD36 receptor levels can be ascribed to the outcomes of stem cell differentiation. As microglial differentiation takes place, it is accompanied by an increase in the CD36 cell receptor. This chain of events ultimately contributes to the diminishment of amyloid plaques and the subsequent improvement of cognitive function in the Alzheimer's disease model (19, 24). The current study exhibits specific limitations, with the most significant among them being the escalation in costs linked to laboratory equipment and materials, the complexity of working with rats, including the challenges of conducting animal surgeries and managing the post-surgery recovery period.

In conclusion, the present study demonstrated that MSC therapy had a remarkable effect on the lncRNA TUSC7/ miR-449a / PPARγ axis in AD rat model as well as the protein level of CD36 which could ultimately lead to the removal of Aβ plaques from the brain tissue of rats with AD and improve spatial cognitive behavior. Transplantation of stem cells alters the pathological condition of the disease by influencing

[DOI: 10.22088/IJMCM.BUMS.12.2.108]

different types of cells, such as neurons, oligodendrocytes, astrocytes, and microglia, in the hippocampus and improving numerous biochemical pathways. Although there are limitations that need to be overcome.

Acknowledgments

The authors would like to thank the Ahvaz Jundishapur University of Medical Sciences, Ahvaz, Iran. This article was derived from the master's thesis of Seyedeh Pardis Pezeshki and financially supported by Ahvaz Jundishapur University of Medical Sciences (Grant No. APRC-0104).

References

1. Lane CA, Hardy J, Schott JM. Alzheimer's disease. Eur J Neurol 2018;25:59-70.

2. Liu S, Suzuki H, Ito H, et al. Serum levels of proteins involved in amyloid-beta clearance are related to cognitive decline and neuroimaging changes in mild cognitive impairment. Alzheimers Dement (Amst) 2019;11:85-97.

3. d'Angelo M, Castelli V, Catanesi M, et al. PPARgamma and Cognitive Performance. Int J Mol Sci 2019;20.

4. Shie FS, Nivison M, Hsu PC, et al. Modulation of microglial innate immunity in Alzheimer's disease by activation of peroxisome proliferator-activated receptor gamma. Curr Med Chem 2009;16:643-51.

5. Yamanaka M, Ishikawa T, Griep A, et al. PPARgamma/RXRalpha-induced and CD36-mediated microglial amyloid-beta phagocytosis results in cognitive improvement in amyloid precursor protein/presenilin 1 mice. J Neurosci 2012;32:17321-31.

6. Stuart LM, Bell SA, Stewart CR, et al. CD36 signals to the actin cytoskeleton and regulates microglial migration via a p130Cas complex. J Biol Chem 2007;282:27392-401.

7. Jones RS, Minogue AM, Connor TJ, et al. Amyloid-beta-induced astrocytic phagocytosis is mediated by CD36, CD47 and RAGE. J Neuroimmune Pharmacol 2013;8:301-11.

8. Luo Q, Chen Y. Long noncoding RNAs and Alzheimer's disease. Clin Interv Aging 2016;11:867-72.

9. Basavaraju M, de Lencastre A. Alzheimer's disease: presence and role of microRNAs. Biomol Concepts 2016;7:241-52.

10. Azizi Dariuni H, Karimi Darabi M, Nazeri Z, et al. Amyloid Beta Alters the Expression of microRNAs Regulating HMGCR and ABCA1 Genes in Astrocytes of C57BL/6J Mice. Int J Mol Cell Med 2023;12:30-9.

11. Yu Y, Zhu M, Zhao Y, et al. Overexpression of TUSC7 inhibits the inflammation caused by microglia activation via regulating miR-449a/PPAR-gamma. Biochem Biophys Res Commun 2018;503:1020-6.

12. Alipour M, Nabavi SM, Arab L, et al. Stem cell therapy in Alzheimer's disease: possible benefits and limiting drawbacks. Mol Biol Rep 2019;46:1425-46.

13. Hernandez AE, Garcia E. Mesenchymal Stem Cell Therapy for Alzheimer's Disease. Stem Cells Int 2021;2021:7834421.

14. Kolios G, Moodley Y. Introduction to stem cells and regenerative medicine. Respiration 2013;85:3-10.

15. Kim J, Lee Y, Lee S, et al. Mesenchymal Stem Cell Therapy and Alzheimer's Disease: Current Status and Future Perspectives. J Alzheimers Dis 2020;77:1-14.

16. Park D, Yang G, Bae DK, et al. Human adipose tissue-derived mesenchymal stem cells improve cognitive function and physical activity in ageing mice. J Neurosci Res 2013;91:660-70.

17. Salem AM, Ahmed HH, Atta HM, et al. Potential of bone marrow mesenchymal stem cells in management of Alzheimer's disease in female rats. Cell Biol Int 2014;38:1367-83.

18. Muniswami DM, Tharion G. Therapeutic Effect of Cell Transplantation and Chondroitinase in Rat Spinal Cord Injury. Int J Appl Basic Med Res 2018;8:220-6.

[DOI: 10.22088/IJMCM.BUMS.12.2.108]

19. Zhang J, Ke KF, Liu Z, et al. Th17 cell-mediated neuroinflammation is involved in neurodegeneration of abeta1-42-induced Alzheimer's disease model rats. PLoS One 2013;8:e75786.

20. Navabi SP, Sarkaki A, Mansouri E, et al. The effects of betulinic acid on neurobehavioral activity, electrophysiology and histological changes in an animal model of the Alzheimer's disease. Behav Brain Res 2018;337:99-106.

21. Cheraghzadeh M, Hanaee-Ahvaz H, Khirolah A, et al. Platelet-rich plasma accelerates bone differentiation in human adipose-derived mesenchymal stromal cells: an experimental study. Iran Red Crescent Med J 2018.

22. Naaldijk Y, Jager C, Fabian C, et al. Effect of systemic transplantation of bone marrow-derived mesenchymal stem cells on neuropathology markers in APP/PS1 Alzheimer mice. Neuropathol Appl Neurobiol 2017;43:299-314.

23. Kan I, Barhum Y, Melamed E, et al. Mesenchymal stem cells stimulate endogenous neurogenesis in the subventricular zone of adult mice. Stem Cell Rev Rep 2011;7:404-12.

24. Ricciarelli R, D'Abramo C, Zingg JM, et al. CD36 overexpression in human brain correlates with beta-amyloid deposition but not with Alzheimer's disease. Free Radic Biol Med 2004;3.

[DOI: 10.22088/IJMCM.BUMS.12.2.108]